The A53T Mutation in α-Synuclein Enhances Proinflammatory Activation in Human Microglia Upon Inflammatory Stimulus

Marine Krzisch, Bingbing Yuan, Wenyu Chen, Tatsuya Osaki, Dongdong Fu, Carrie M. Garrett-Engele, Devon S. Svoboda, Kristin R. Andrykovich, Michael D. Gallagher, Mriganka Sur, and Rudolf Jaenisch

ABSTRACT

BACKGROUND: Parkinson's disease (PD) is the second most common neurodegenerative disease, following Alzheimer's. It is characterized by the aggregation of α-synuclein into Lewy bodies and Lewy neurites in the brain. Microglia-driven neuroinflammation may contribute to neuronal death in PD; however, the exact role of microglia remains unclear and has been understudied. The A53T mutation in the gene coding for α-synuclein has been linked to early-onset PD, and exposure to A53T mutant human α-synuclein increases the potential for inflammation of murine microglia. To date, its effect has not been studied in human microglia.

METHODS: Here, we used 2-dimensional cultures of human pluripotent stem cell–derived microglia and transplantation of these cells into the mouse brain to assess the cell autonomous effects of the A53T mutation on human microglia.

RESULTS: We found that A53T mutant human microglia had an intrinsically increased propensity toward proinflammatory activation upon inflammatory stimulus. Additionally, transplanted A53T mutant microglia showed a strong decrease in catalase expression in noninflammatory conditions and increased oxidative stress.

CONCLUSIONS: Our results indicate that A53T mutant human microglia display cell autonomous phenotypes that may worsen neuronal damage in early-onset PD.

https://doi.org/10.1016/j.biopsych.2024.07.011

Microgliosis is an early and sustained response in Parkinson's disease (PD) (1,2), and microglia-driven neuroinflammation may contribute to neuronal death in PD. However, the exact role of microglia remains unclear. The A53T mutation in the α-synuclein gene *SNCA* is associated with autosomal dominant, early-onset PD (3). Exposure of mouse microglia to human A53T mutant α-synuclein promotes their inflammatory responses more strongly than exposure to the wild-type (4). However, to our knowledge, the impact of this mutation on human microglia remains uninvestigated.

Mouse models incompletely mirror PD pathogenesis (5) and have yet to yield a cure. Furthermore, although mouse and human microglia are largely similar, human microglia express genes relevant to human neurodegenerative disease not expressed by other mammals (6). Therefore, there is a need to study human-relevant pathways using human microglia.

Conventional culture methods fall short of replicating human microglia physiology (7,8). In contrast, myeloid precursors (MPs) derived from human pluripotent stem cells (hPSCs) and transplanted into the brain of immune-deprived mice colonize the mouse brain and yield microglia that retain their human identity and more closely resemble ex vivo human microglia than in vitro 2-dimensional cultures (9–12). Therefore,

transplantation of human MPs carrying PD-related mutations in the mouse brain may yield new, more physiologically relevant insights into the dysfunction of microglia in PD.

Here, we used both the transplantation of A53T mutant (PD) hPSC-derived MPs and isogenic controls into mice and their differentiation into microglia in vitro to characterize the effects of the A53T mutation on human microglia.

METHODS AND MATERIALS

See Supplemental Methods in Supplement 1 for detailed information on all methods.

Experimental Animals

We used Rag2/IL2rg double knockout mice expressing the human allele of *CSF1*.

hPSC Culture and Labeling

We used hPSC lines carrying the A53T mutation in α-synuclein and control cell lines previously generated and characterized by our group, listed in Table S1 in Supplement 1 (13). They were targeted with GFP (green fluorescent protein) at the AAVS1 locus as previously described (14). To prevent accidental inversion of the cell lines, the A53T mutation was

genotyped before starting each differentiation (Tables S2 and S3 in Supplement 1).

In Vitro Differentiation of Microglia and Stimulation With Lipopolysaccharide and Interferon Gamma

In vitro differentiation of microglia was performed using the modified version of a published protocol (15). On day 29 of differentiation, cultured cells were stimulated using lipopolysaccharide (LPS) (5 μg/mL) and interferon gamma (IFN-γ) (20 ng/mL).

MP Differentiation and Transplantation

hPSCs were differentiated into MPs using the modified version of a previously published protocol (16) and transplanted on postnatal day 0 (P0) to P3 into mouse pups of both sexes.

LPS Injections in Transplanted Mice

Two months after transplantation, the mice received a single intraperitoneal injection of LPS (Sigma-Aldrich L2630) dissolved in sterile saline (5 mg/kg). Animals were euthanized 24 hours after the injection, and brains were harvested.

Transplanted Cell Extraction for RNA Sequencing

Transplanted cells were extracted from the mouse brains as previously described (10).

Sample Fixation and Immunofluorescence Staining

Cultured microglia and mouse brains were fixed using 4% paraformaldehyde. Immunostainings were performed using antibodies listed in Tables S4 and S5 in Supplement 1.

Detection of Oxidative Stress, Apoptosis, and Senescence in Cultured Human Microglia

Oxidative stress was measured using the CellROX Orange Reagent (Invitrogen). Apoptosis was detected using the CellEvent™ Caspase 3/7 Red detection reagent (Invitrogen). Cellular senescence was assessed using the Cellular Senescence Assay Kit (Merck-Millipore).

Fluorescence Imaging and Analyses

We used Zeiss confocal microscopes to acquire confocal images and an EVOS epifluorescence microscope for epifluorescence images.

Statistical Analyses of Microscopy

Statistical analyses were performed using GraphPad Prism version 9 (GraphPad Software; http://www.graphpad.com).

RESULTS

Human A53T Mutant Microglia Display Gene Signatures That Suggest an Altered State of Activation

To generate hypotheses about the impact of the SNCA A53T mutation on human microglia, we first performed bulk RNA sequencing on PD and isogenic control cultured microglia. Most cultured cells (81%–98%) were Iba1 and P2RY12 positive on day 29 of differentiation, confirming successful differentiation into human microglia across all cell lines (Figure 1A

and Table 1). RNA from 3 independent in vitro microglia differentiations per cell line was pooled at equal weight to generate 6 samples, each representing a cell line. We assessed the expression of key microglial genes (7,10) in cultured microglia. Most of these genes were expressed at high levels, with no differences detected in their expression levels between PD and control microglia (Figure S1A in Supplement 1). This confirmed the successful differentiation and similar differentiation stages of PD and control microglia, indicating that observed differences between PD and control microglia were unlikely to be due to different stages of differentiation.

The impact of the A53T mutation on SNCA expression levels is unclear in the literature (17–19). Here, neither the A53T mutation nor its correction altered SNCA gene expression levels in microglia (Figure S1B in Supplement 1). Gene set enrichment analysis revealed significant alterations in pathways related to immune response, inflammation, microglia activation, and immunomodulation in PD microglia (Figure 1B; Tables S6–S9 in Supplement 2). Pathways associated with cell cycle were upregulated, and pathways related to cell death, senescence, and aging showed differential expression (Figure 1B; Tables S6–S9 in Supplement 2). The following genes involved in immunomodulation were among the 10 most downregulated genes in PD microglia: FCGR2B, NOTCH4, CD200R1, and SEMA3C (Figure 1C and Table 2). The following genes involved in immune response and associated with inflammatory diseases were among the 10 most upregulated genes in PD microglia: RETN, MCEMP1, SLC11A1, MAPK13, and MSR1 (Figure 1C and Table 3). Together, these results suggested an altered state of activation, increased proliferation, and increased cellular senescence of PD microglia.

Primary microglia cultured in a dish lose their microglia-specific gene signatures and start expressing genes related to inflammation after 6 hours in culture (7). Transplanting human MPs into the mouse brain supports microglial differentiation and largely overcomes this limitation. To study the altered activation state of PD microglia in a more physiologically relevant setting, we transplanted PD hPSC–derived or isogenic control MPs into the mouse brain, allowing them to mature into microglia within an in vivo–like environment (Figure 2A). By 2 months postinjection (PI), the transplanted cells had successfully populated the mouse brain (Figure 2B), and 93% to 100% of the cells were Iba1 and P2RY12 positive (Figure 2C and Table 4), confirming their successful differentiation into human microglia.

At 2 months PI, PD and isogenic control microglia were extracted from the mouse brains, and RNA sequencing was performed. RNA from transplanted cells extracted from 2 or 3 chimeras per cell line was pooled at equal weight. Similar to cultured microglia, transplanted PD microglia showed similar SNCA expression levels compared with control microglia (Figure S1C in Supplement 1). No consistent differences were observed in the intracellular levels of α-synuclein between control and PD cultured (Figure S1D in Supplement 1) or transplanted (Figure S1E in Supplement 1) microglia. Immunostaining revealed low levels of α-synuclein in transplanted human microglia, consistent with the literature (20), and no evidence of α-synuclein aggregation in PD microglia (Figure S1F, G in Supplement 1). PD and control microglia
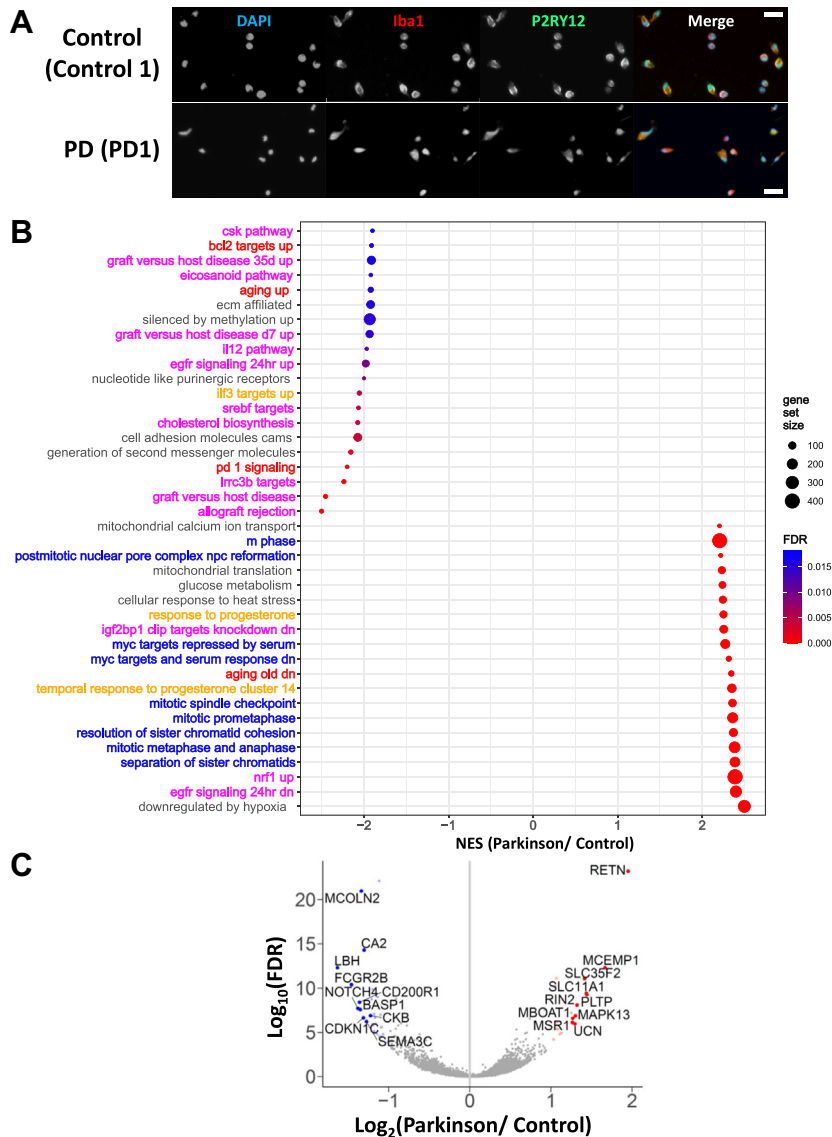
Figure 1. Bulk RNA sequencing analysis of human pluripotent stem cell–derived microglia differentiated in vitro shows differential expression of gene pathways linked to inflammation, immunomodulation, cell cycle, and cellular senescence in PD microglia compared with isogenic control microglia. **(A)** Epifluorescence microscopy pictures of 2-dimensional cultures of control (control 1 cell line, upper panel) and PD (PD 1 cell line, lower panel) human pluripotent stem cell–derived microglia at 29 days in vitro, immunostained with DAPI (blue), Iba1 (red), and P2RY12 (magenta). Scale bars = 20 μm. **(B)** Upregulated and downregulated pathways in PD vs. isogenic control in vitro differentiated microglia as assessed by gene set enrichment analysis. For clarity, only select pathways are shown. The exhaustive list of pathways can be found in Tables S6–S9 in Supplement 2. An NES > 0 indicates upregulation of the pathway (lower panel), whereas an NES < 0 indicates downregulation of the pathway (upper panel) in PD microglia. The FDR threshold was set at .05. Gene pathways involved in immune response, inflammation, and microglia activation are shown in magenta. Gene pathways involved in senescence and aging are shown in red. Gene pathways linked to immunomodulation are shown in orange. Gene pathways involved in cell cycle and cell proliferation are shown in blue. **(C)** Volcano plot showing upregulated and downregulated genes in PD vs. control in vitro differentiated microglia. The differentially expressed genes with an adjusted p value < .05 and at least 2-fold differences are highlighted in red (upregulated genes) and blue (downregulated genes), and gene symbols for the top 10 genes are labeled. n = 3 biological experiments for each cell line. FDR, false discovery rate; NES, normalized enrichment score; PD, Parkinson's disease.

expressed most key microglial genes at high and similar levels (Figure S1H in Supplement 1). This confirmed the successful differentiation and similar differentiation stages of PD and

Table 1. All the Cell Lines Have Successfully Differentiated Into Microglia at 29 Days In Vitro

Cell Line	% Iba1+ P2RY12+ Cells
Control 1	86 ± 3.2
PD 1	94 ± 1.6
Control 2	98 ± 0.0
PD 2	98 ± 1.1
Control 3	81 ± 0.7
PD 3	95 ± 1.7

Percentages of Iba1-P2RY12 double-positive cells per cell line. n = 3 independent experiments per cell line, 32 to 67 cells per experiment.

PD, Parkinson's disease.

control transplanted microglia, indicating that observed differences between PD and control microglia were unlikely to be due to different stages of differentiation. No consistent differences in the overall density and distribution of GFP-positive transplanted cells were observed between control and PD microglia (Figure S2 in Supplement 1).

To validate our cultured microglia–driven hypotheses regarding disease-relevant pathways of PD microglia, we assessed the differentially expressed pathways in transplanted PD microglia versus control microglia. Gene set enrichment analysis indicated differential expression of pathways involved in translation, metabolism, immune response, inflammation, and microglia activation in PD microglia, as well as a downregulation of pathways involved in immunomodulation and DNA repair. In contrast to findings in cultured microglia, pathways linked to cell cycle and proliferation were

Table 2. Ten Most Downregulated Genes in In Vitro Differentiated PD Microglia Compared With Isogenic Control Microglia

Gene Symbol	Gene Name	Gene Ontology	Log$_2$(FC)
LBH	LBH regulator of Wnt signaling pathway	Negative regulation of transcription	−1.6
FCGR2B	Fc gamma receptor IIb	Inhibitory receptor of immune cells; inhibits microglia activation[a]	−1.5
NOTCH4	Notch receptor 4	Anti-inflammatory activity in activated macrophages[a]	−1.4
CD200R1	CD200 receptor 1	Inhibition of the secretion of proinflammatory molecules by microglia; stimulation results in neuroprotection in a model of PD[a]	−1.4
BASP1	Brain abundant membrane attached signal protein 1	Membrane-bound protein	−1.3
MCOLN2	Mucolipin TRP cation channel 2	Possible role in innate immune response[a]	−1.3
CDKN1C	Cyclin dependent kinase inhibitor 1C	Negative regulator of cell proliferation	−1.3
CA2	Carbonic anhydrase 2	Increased in aging and neurodegeneration[a]	−1.3
SEMA3C	Semaphorin 3C	Induces apoptosis of activated proinflammatory microglia[a]	−1.3
CKB	Creatine kinase B	Suppresses ferroptosis; ferroptosis may contribute to neurodegeneration[a]	−1.2

n = 3 cell lines per group, 3 independent experiments per cell line.
FC, fold change; PD, Parkinson's disease.
[a]Gene ontologies of particular interest.

downregulated in PD transplanted microglia. Pathways associated with cell death, senescence, and aging were differentially expressed in PD transplanted microglia compared with control microglia (Figure 3A; Tables S10–S13 in Supplement 2).

The most differentially expressed gene in PD transplanted microglia was *CAT*, encoding catalase, which was strongly downregulated (Figure 3B and Table 5). The *CAT* gene was also significantly downregulated in in vitro cultures, although to a lesser extent: log$_2$ fold change(PD/control) = −0.2, $p_{adjusted}$ = .04. Catalase mitigates oxidative stress by breaking down reactive oxygen species (ROS) (21). The 10 most significantly upregulated genes in PD microglia included *RBMS3*, linked to motor complications in PD (22) (Table 6). Together, these results suggested that human PD microglia differentiated in the

more physiological context of the mouse brain may exhibit increased protein translation, metabolism, proinflammatory activation, and oxidative stress and decreased cell division. The differential expression of cell death, senescence, and aging pathways and the downregulation of pathways involved in DNA repair and cell cycle suggested that PD transplanted microglia might also display increased cellular senescence.

To compare gene expression changes in A53T mutant microglia with those in idiopathic PD, we analyzed the overlap between our RNA sequencing results and previously published single-cell RNA sequencing data from the midbrain of patients with idiopathic PD compared with age- and sex-matched control participants (23). We extracted microglial gene expression levels from the deposited dataset and performed

Table 3. Ten Most Upregulated Genes in In Vitro Differentiated PD Microglia Compared With Isogenic Control Microglia

Gene Symbol	Gene Name	Gene Ontology	Log$_2$(FC)
RETN	Resistin	Involved in immune defense[a]	2.0
MCEMP1	Mast cell expressed membrane protein 1	Predicted to be involved in regulating immune response[a]	1.7
PLTP	Phospholipid transfer protein	Increased in AD; deletion increases microglial phagocytosis and reduces cerebral amyloid-β deposition in a mouse model of AD[a]	1.4
SLC11A1	Solute carrier family 11 member 1	Involved in protection against ROS in macrophages; associated with inflammatory diseases[a]	1.4
SLC35F2	Solute carrier family 35 member F2	Predicted to enable transmembrane transporter activity	1.4
RIN2	Ras and Rab interactor 2	Involved in membrane trafficking in the early endocytic pathway	1.3
MAPK13	Mitogen-activated protein kinase 13	Contributes to inflammation by promoting cytokine release by microglia[a]	1.3
UCN	Urocortin	Inhibits microglia activation[a]	1.3
MBOAT1	Membrane-bound O-acyltransferase domain containing 1	Transfers organic compounds to hydroxyl groups of protein targets in membranes	1.3
MSR1	Macrophage scavenger receptor 1	Secretion of proinflammatory cytokines by macrophages; involved in the uptake and clearance of soluble amyloid-β in AD by microglia[a]	1.3

n = 3 cell lines per group, 3 independent experiments per cell line.
AD, Alzheimer's disease; FC, fold change; PD, Parkinson's disease; ROS, reactive oxygen species.
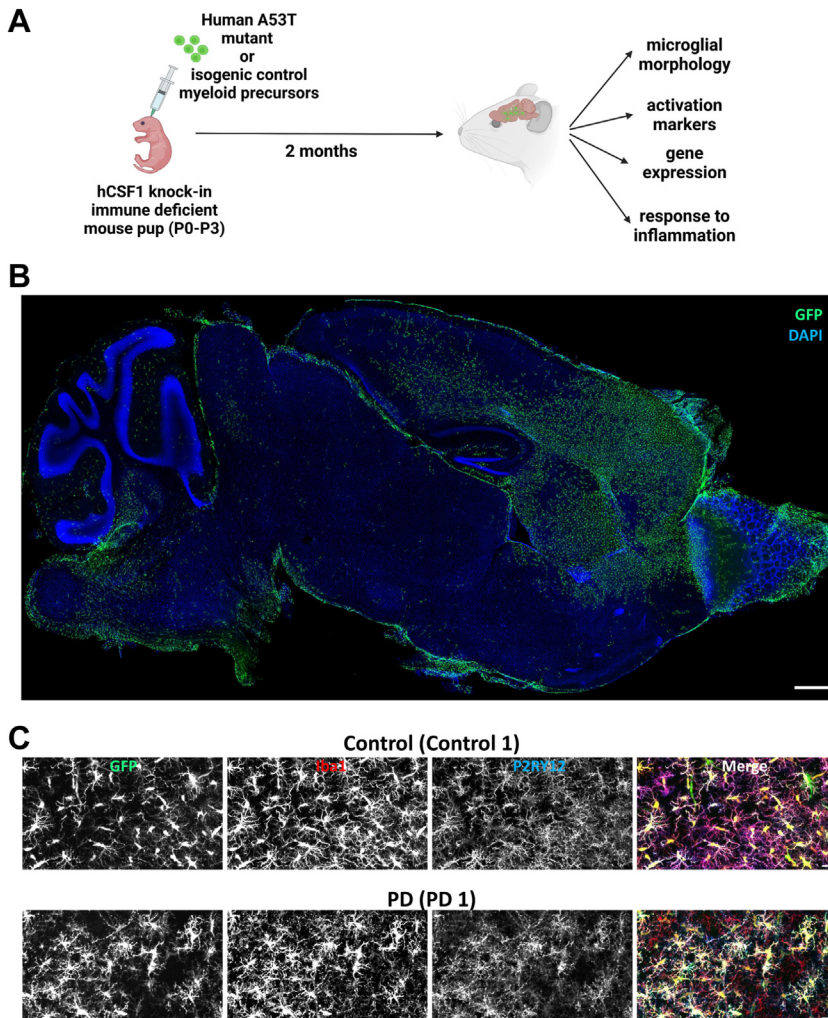[a]Gene ontologies of particular interest.

Figure 2. Transplanted hPSC-derived MPs have populated the mouse brain and differentiated into microglia at 2 months posttransplantation. **(A)** Experimental design. For each isogenic pair of hPSC lines, one cohort of immune-deficient neonatal mouse pups was injected with PD hPSC-derived MPs, and another cohort was injected with isogenic control hPSC-derived MPs. Mouse brains were analyzed at 2 months post-injection. **(B)** Tile scan confocal maximum-intensity projection of a 100-μm-thick sagittal brain slice of a mouse transplanted with control (control 1) MPs at 2 months postinjection. Scale bar = 500 μm. Green: GFP-labeled hPSC-derived microglia, blue: DAPI. **(C)** Confocal maximum-intensity projection of transplanted control (upper panel, control 1 cell line) and PD (lower panel, PD 1 cell line) MPs at 2 months postinjection, immunostained for microglia markers. Red: Iba1; green: GFP; blue: P2RY12. Scale bars = 20 μm. GFP, green fluorescent protein; hPSC, human pluripotent stem cell; MP, myeloid precursor; P, postnatal day; PD, Parkinson's disease.

pseudo-bulk analysis using DESeq2. Comparing the log_2 fold changes between disease and control groups for A53T mutant microglia and idiopathic PD, we found a correlation close to 0 (Figure S3 in Supplement 1). Few differentially expressed genes

Table 4. All the Cell Lines Have Successfully Differentiated Into Microglia at 2 Months After Transplantation Into the Mouse Brain

Cell Line	% Iba1+ P2RY12+ Cells
Control 1	93 ± 4.5
PD 1	100 ± 0.0
Control 2	94 ± 3.5
PD 2	97 ± 2.9
Control 3	100 ± 0.0
PD 3	89 ± 0.7

Percentages of Iba1-P2RY12 double-positive cells per cell line. n = 3 animals per cell line, 41–219 cells per animal.

PD, Parkinson's disease.

were shared between A53T mutant human transplanted microglia and idiopathic PD microglia (Table 7; Figure S3 in Supplement 1). Idiopathic PD microglia did not show changes in *CAT* gene expression. However, similar to findings in A53T mutant human transplanted microglia and consistent with midbrain microgliosis described in that study, gene set enrichment analysis revealed differential expression of pathways involved in immune response, inflammation, microglia activation, immune modulation, and cellular senescence in idiopathic PD microglia (Figure S4 in Supplement 1). Pathways linked to cell cycle were upregulated in microglia from patients with idiopathic PD.

Human A53T Mutant Microglia Show Increased Proinflammatory Activation in Proinflammatory Conditions

Iba1 is a widely used marker of microglial activation (24). We first assessed microglia activation in cultured microglia using Iba1 staining (Figure S5 in Supplement 1). Mature cultured microglia were stimulated with LPS and IFN-γ (LPS+IFN) for
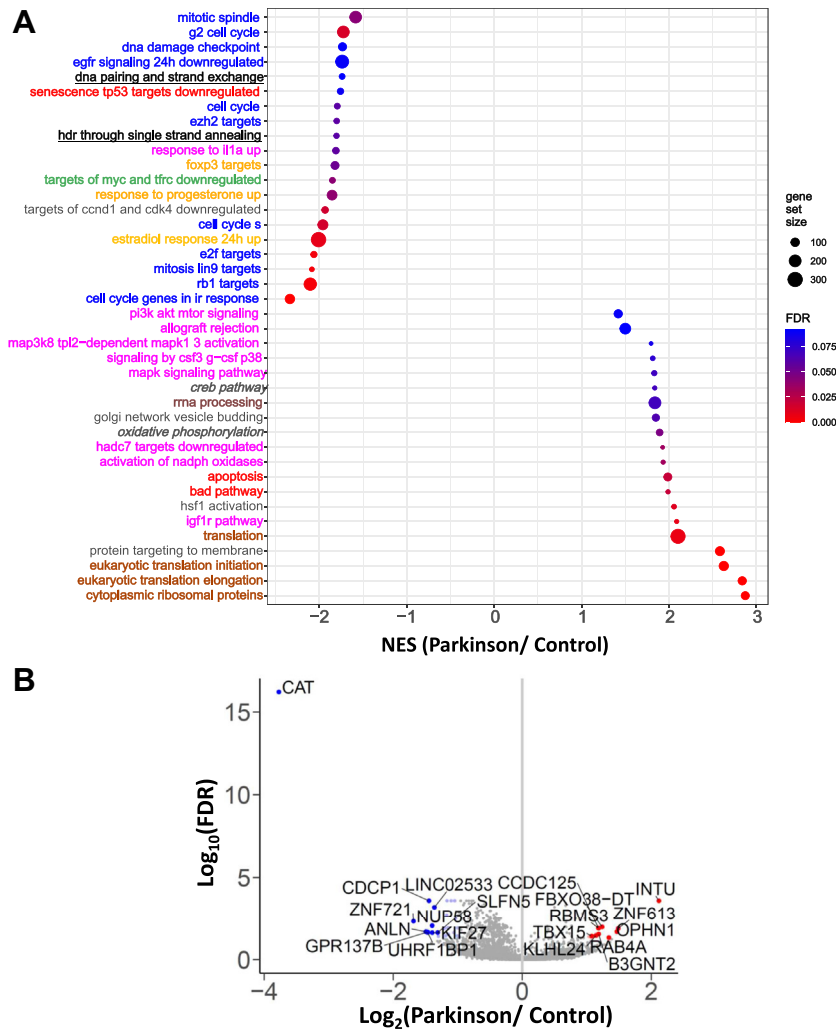
Figure 3. Bulk RNA sequencing analysis of human pluripotent stem cell–derived microglia transplanted into the brain of mice shows differential expression of gene pathways linked to inflammation, microglia activation, immune response, immunomodulation, protein translation, metabolism, cell cycle, DNA repair, and cellular senescence in PD microglia compared with isogenic control microglia. **(A)** Upregulated and downregulated pathways in PD vs. isogenic control transplanted microglia as assessed by gene set enrichment analysis. For clarity, only select pathways are shown. The exhaustive list of pathways can be found in Tables S10–S13 in Supplement 2. An NES > 0 indicates upregulation of the pathway (lower panel), whereas an NES < 0 indicates downregulation of the pathway (upper panel) in PD transplanted microglia. The FDR threshold was set at .1. Gene pathways involved in immune response, inflammation, and microglia activation are shown in magenta. Gene pathways involved in cell death, senescence, and aging are shown in red. Gene pathways linked to immunomodulation are shown in orange. Gene pathways involved in cell cycle and cell proliferation are shown in blue. Gene pathways involved in translation are shown in brown. Gene pathways involved in DNA repair are shown in black, underlined. Gene pathways linked to metabolism are shown in black, italic. A gene pathway involved in cell cycle arrest is shown in green. **(B)** Volcano plot showing upregulated and downregulated genes in PD vs. control transplanted microglia. The differentially expressed genes with an adjusted p value < .05 and at least 2-fold differences are highlighted in red (upregulated genes) and blue (downregulated genes), and gene symbols for the top 10 genes are labeled. n = 2–3 transplanted brains per cell line. FDR, false discovery rate; NES, normalized enrichment score; PD, Parkinson's disease.

24 hours or left untreated. In noninflammatory conditions (untreated cocultures), no consistent differences in Iba1 staining intensity were observed between control and PD microglia (Figure S5A, B, D in Supplement 1). In proinflammatory conditions (LPS+IFN), PD cultured microglia showed higher Iba1 staining intensity than control microglia, indicating higher activation levels (Figure S5A, C, D in Supplement 1).

To validate our in vitro results, we performed immunofluorescence analyses on transplanted mouse brain slices at 2 months PI. We focused on transplanted microglia in the mouse striatum because it was consistently populated with human microglia in transplanted mice and is involved in PD (25). During activation, microglia undergo morphological changes. Quiescent microglia have a complex, ramified morphology. Activated microglia display thickened and retracted branches, appearing bushy, with fewer primary processes and ramifications. As activation progresses, they transition to an ameboid shape (26). CD68 labels lysosomes and is a widely used marker for microglia activation due to increased expression in activated microglia (24). p65 is a subunit

of the nuclear factor-κB (NF-κB) complex, which targets genes involved in inflammation progression (27). The canonical NF-κB p65/p50 pathway is activated in postmortem PD human brains and the substantia nigra of animals undergoing dopaminergic neuron degeneration (28). Additionally, NF-κB canonical pathway activation induces microglia proinflammatory activation and motor neuron death via inflammatory pathways (29).

First, we separated microglia into different categories based on morphology, following a methodology similar to that of previous studies on microglia activation (30,31) (Figure 4A). Ramified microglia displayed small cell bodies with numerous ramifications. Bushy I microglia had enlarged cell bodies, with fewer processes. Bushy II microglia had enlarged cell bodies with fewer than 10 primary processes. Ameboid microglia had round, enlarged cell bodies, with fewer than 3 primary processes. Then, we quantified percentages of CD68-positive and p65-positive PD and isogenic control transplanted microglia and the staining intensity of Iba1 in PD and control transplanted microglia. In noninflammatory conditions (no LPS injection),

Table 5. Ten Most Downregulated Genes in Transplanted PD Microglia Compared With Isogenic Control Microglia

Gene Symbol	Gene Name	Gene Ontology	Log$_2$(FC)
CAT	Catalase	Activity decreased in brains of patients with PD[a] Mitigates oxidative stress by breaking down ROS[a]	−3.8
ZNF721	Zinc finger protein 721	Transcription factor	−1.7
ANLN	Anillin, actin binding protein	Cell growth and migration, cytokinesis	−1.5
UHRF1BP1	UHRF1 binding protein 1	Enables histone deacetylase binding activity and identical protein binding activity	−1.5
GPR137B	G protein–coupled receptor 137B	Positive regulation of TORC1 signaling; positive regulation of protein localization to lysosome and lysosome morphology and regulation of GTPase activity	−1.5
CDCP1	CUB domain containing protein 1	Involved in cell adhesion; cell matrix association; and T-cell activation, migration, and chemotaxis	−1.4
NUP58	Nucleoporin 58	Component of the nuclear pore complex	−1.4
KIF27	Kinesin family member 27	Potential role in Hedgehog signaling pathway	−1.4
SLFN5	Schlafen family member 5	Predicted to be involved in cell differentiation	−1.3
PLAU	Plasminogen activator, urokinase	May be associated with late-onset Alzheimer's disease	−1.3

n = 3 cell lines per group, 3 independent experiments per cell line.

FC, fold change; PD, Parkinson's disease; ROC, reactive oxygen species.

[a]Gene ontologies of particular interest.

striatal PD microglia were largely quiescent, as assessed by low percentages of CD68-positive cells and high percentages of ramified cells (Figure 4B, C, E, F; Figure S6A, B in Supplement 1). The morphology and percentage of CD68-positive cells were similar in control and PD microglia (Figure 4B, C, F; Figure S6A, B in Supplement 1). No consistent differences in Iba1 staining intensity (Figure 4G, H; Figure S6C in Supplement 1) or percentage of p65-positive cells were observed between control and PD microglia (Figure 4I, J; Figure S6D in Supplement 1). Therefore, in noninflammatory conditions, the activation levels of PD and control microglia were similar.

LPS is a potent stimulator of microglia and has been used to study inflammation in PD pathogenesis (32). Intraperitoneal LPS injection successfully activates human microglia transplanted into the mouse brain (10,11). To place transplanted microglia in inflammatory conditions, transplanted mice were injected with LPS at 5 mg/kg and analyzed 24 hours PI. LPS successfully induced activation of control and PD microglia, as assessed by elevated percentages of CD68-positive cells and a shift toward less ramified morphologies compared with noninflammatory conditions (Figure 4B–F; Figure S7A, B in Supplement 1). Transplanted PD microglia's morphological distribution was significantly shifted toward less ramified categories compared with control microglia (Figure 4B, D; Figure S7A in Supplement 1), and they displayed slightly but significantly increased percentages of CD68-positive cells (Figure 4E, F; Figure S7B in Supplement 1). Moreover, PD microglia showed increased Iba1 staining

Table 6. Ten Most Upregulated Genes in Transplanted PD Microglia Compared With Isogenic Control Microglia

Gene Symbol	Gene Name	Gene Ontology	Log$_2$(FC)
INTU	Inturned planar cell polarity protein	Key role in ciliogenesis and embryonic development	2.1
ZNF613	Zinc finger protein 613	Transcription factor	1.5
OPHN1	Oligophrenin 1	Implicated in synaptic function	1.5
RAB4A	RAB4A, member RAS oncogene family	Associated with early endosomes and is involved in their sorting and recycling; involved in AD	1.3
FBXO38-DT	FBXO38 divergent transcript	Long noncoding RNA	1.2
B3GNT2	UDP-GlcNAc:betaGal beta-1,3-*N*-acetylglucosaminyltransferase 2	Transmembrane protein	1.2
RBMS3	RNA binding motif single stranded interacting protein 3	Implicated in DNA replication, gene transcription, cell cycle progression, and apoptosis; linked to AD and to motor complications in PD[a]	1.2
CCDC125	Coiled-coil domain containing 125	Negative regulation of cell motility	1.2
KLHL24	Kelch like family member 24	Ubiquitin ligase substrate receptor	1.1
TBX15	T-box transcription factor 15	Transcription factor regulating developmental processes	1.1

n = 3 cell lines per group, 3 independent experiments per cell line.

AD, Alzheimer's disease; FC, fold change; PD, Parkinson's disease.

[a]Gene ontologies of particular interest.

Table 7. Shared Differentially Expressed Genes Between A53T Mutant Transplanted Microglia and Microglia From the Midbrain of Patients With Idiopathic PD

Gene Symbol	Gene Name	Gene Ontology	Log$_2$(FC), A53T Mutant	Log$_2$(FC), Idiopathic PD
ANLN	Anillin, actin binding protein	Cell growth and migration, cytokinesis	−1.5	−1.5
SYT11	Synaptotagmin 11	Inhibits cytokine release and phagocytosis in microglia, mediator of Parkinson-linked neurotoxicity[a]	−1.2	−1.4
GPM6A	Glycoprotein M6A	Neuron migration and stem cell differentiation	−1.2	−1.3
ABCA5	ATP-binding cassette subfamily A member 5	Reduces amyloid-β peptide production, expression associated with decreased risk of PD[a]	−1.0	−1.1

FC, fold change; PD, Parkinson's disease.
[a]Gene ontologies of particular interest.

intensity (Figure 4G, H; Figure S7C in Supplement 1) and higher percentages of p65-positive cells (Figure 4I, J; Figure S7D in Supplement 1) post-LPS induction. Therefore, while PD and control microglia exhibited similar levels of activation in noninflammatory conditions, when placed in proinflammatory conditions, transplanted PD microglia showed increased
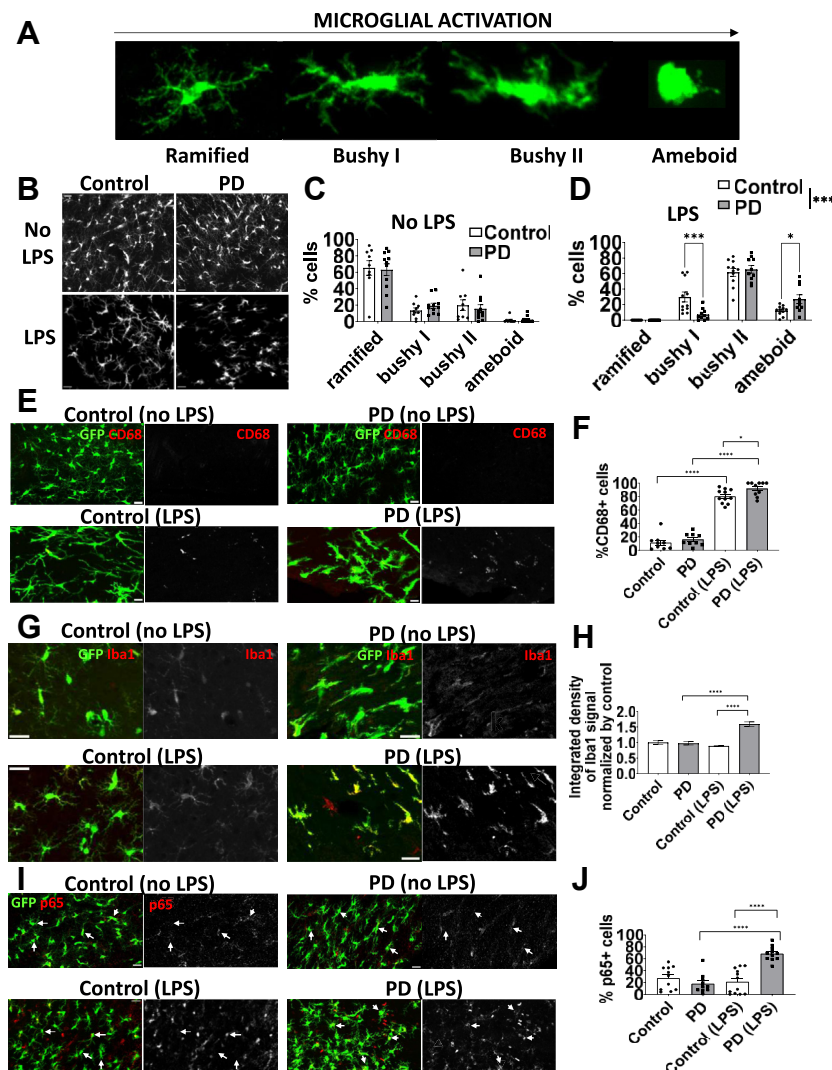

Figure 4. Transplanted striatal PD microglia display increased proinflammatory activation compared with isogenic control microglia in proinflammatory conditions. **(A)** Confocal maximum-intensity projections illustrating the classification of transplanted human microglia into different morphological categories. Ramified microglia had a small cell body and a high number of ramifications. Bushy I microglia had enlarged cell bodies, with fewer processes. Bushy II microglia had enlarged cell bodies with <10 primary processes. Ameboid microglia had round, enlarged cell bodies with <3 primary processes. **(B)** Confocal microscopy maximum-intensity projections of GFP-labeled control and PD transplanted striatal microglia in noninflammatory (no LPS injection, upper panel) and proinflammatory (LPS injection, lower panel) conditions. Scale bars = 20 μm. Percentages of ramified, bushy I, bushy II, and ameboid cells in PD and control transplanted striatal microglia in noninflammatory **(C)** and proinflammatory (LPS injection) **(D)** conditions. Repeated-measures mixed-effects analysis followed by Sidak's multiple comparisons test. **(E)** Confocal maximum-intensity projections of control and PD GFP-labeled transplanted striatal microglia in noninflammatory (no LPS injection, upper panel) or proinflammatory (LPS injection, lower panel) conditions, immunostained with CD68 (red). Scale bars = 20 μm. **(F)** Percentage of CD68$^+$ cells in transplanted PD and control striatal microglia in noninflammatory and proinflammatory (LPS) conditions. Unpaired Mann-Whitney tests. **(G)** Confocal maximum-intensity projections of control and PD GFP-labeled transplanted striatal microglia in noninflammatory (no LPS injection, upper panel) or proinflammatory (LPS injection, lower panel) conditions, immunostained with Iba1 (red). Scale bars = 20 μm. **(H)** Integrated densities of Iba1 signal of control and PD microglia normalized by control values in noninflammatory and proinflammatory (LPS) conditions. Unpaired Mann-Whitney tests. **(I)** Confocal maximum-intensity projections of control and PD GFP-labeled transplanted striatal microglia in noninflammatory (no LPS injection, upper panel) or proinflammatory (LPS injection, lower panel) conditions, immunostained with p65 (red). Scale bars = 20 μm. **(J)** Percentage of p65-positive cells in transplanted PD and control striatal microglia in noninflammatory and proinflammatory (LPS) conditions. Unpaired Mann-Whitney test and unpaired t test. n = 3 cell lines per group, 3–5 transplanted mice per cell line. Data are represented as mean ± SEM. *p < .05, ***p < .001, ****p < .0001. GFP, green fluorescent protein; LPS, lipopolysaccharide; PD, Parkinson's disease.
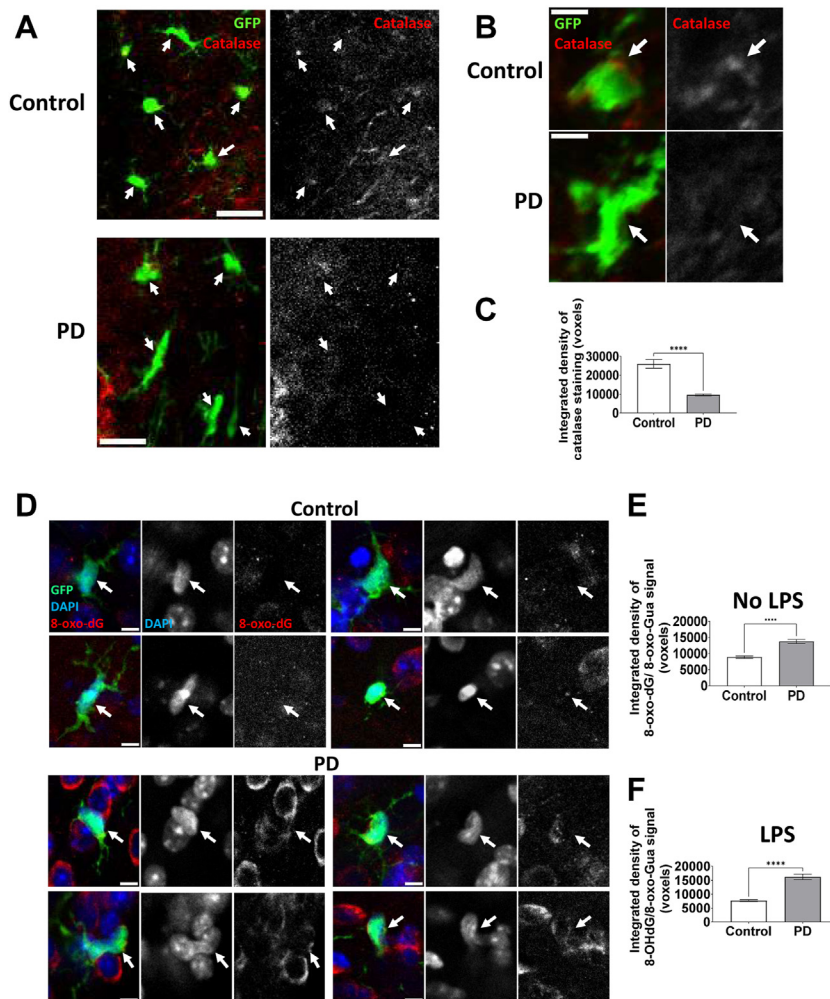
Figure 5. Transplanted PD striatal microglia display strongly decreased catalase expression in noninflammatory conditions and increased oxidative stress. **(A)** Low magnification confocal plans of control and PD transplanted striatal microglia at 2 months PI immunostained for catalase (no LPS challenge). Scale bars = 20 μm. Arrows show cell bodies. **(B)** High magnification confocal plans of control and PD transplanted striatal microglia at 2 months PI immunostained for catalase (no LPS challenge). Scale bars = 5 μm. Arrows show cell bodies. **(C)** Mean integrated density of catalase staining in transplanted control and PD striatal microglia at 2 months PI (no LPS injection). Unpaired Mann-Whitney test. **(D)** Confocal plans of control (upper panel) and PD (lower panel) transplanted striatal microglia at 2 months PI immunostained for 8-oxo-dG/8-oxo-Gua (no LPS injection). Scale bars = 5 μm. Arrows show cell bodies. **(E)** Mean integrated density of 8-oxo-dG/8-oxo-Gua staining in transplanted control and PD striatal microglia at 2 months PI (no LPS challenge). Unpaired Mann-Whitney test. **(F)** Mean integrated density of 8-oxo-dG/8-oxo-Gua staining in transplanted control and PD striatal microglia at 2 months PI after LPS challenge. Unpaired Mann-Whitney test. n = 3 cell lines per group, 3–5 transplanted mice per cell line. Data are represented as mean ± SEM. ****$p < .0001$. GFP, green fluorescent protein; LPS, lipopolysaccharide; PD, Parkinson's disease; PI, postinjection.

proinflammatory activation compared with isogenic control microglia.

Transplanted Human A53T Mutant Microglia Display Decreased Catalase Expression and Increased Oxidative Stress

To confirm decreased expression of catalase in PD transplanted microglia at the protein level, we performed immunofluorescence staining for catalase on brain slices from transplanted mice at 2 months PI. Consistent with the RNA sequencing results, we observed a marked decrease in catalase signal intensity in PD microglia compared with control microglia in noninflammatory conditions (Figure 5A–C; Figure S8A in Supplement 1). To investigate whether this decrease was correlated with increased oxidative stress in PD microglia, we immunostained brain slices from transplanted mice with the DNA and RNA oxidative stress marker 8-oxo-dG/8-oxo-Gua at 2 to 3 months PI. Staining intensity of 8-oxo-dG/8-oxo-Gua was increased, indicating increased oxidative damage in PD transplanted microglia in both noninflammatory

and proinflammatory conditions (Figure 5D–F; Figure S8B, C in Supplement 1). Surprisingly, no consistent difference in catalase expression was observed between PD and control microglia in proinflammatory conditions (Figure S8D in Supplement 1). This was due to a strong upregulation of catalase in PD transplanted microglia, which was absent in control microglia (Figure S8E in Supplement 1). Conversely, no consistent differences in catalase expression were found between control and PD cultured microglia in noninflammatory conditions (Figure S8F in Supplement 1), and no consistent differences in oxidative stress were observed between cultured control and PD microglia in non- or proinflammatory conditions, as assessed using the oxidative stress detection reagent CellROX, which fluoresces upon oxidation by ROS (Figure S9 in Supplement 1).

RNA sequencing data also suggested differences in cellular senescence, cell division, and apoptosis between PD and control microglia. We immunostained transplanted microglia for cleaved caspase 3, an apoptosis marker (Figure S10A–C in Supplement 1), and assessed the apoptosis levels of cultured microglia using a Caspase 3/7 CellEvent assay (Figure S10D–F

in Supplement 1). In both non- and proinflammatory conditions, whether cultured or transplanted, apoptotic microglia percentages were low and similar between PD and control microglia. Next, we immunostained PD and control transplanted and cultured microglia for ki67, a cell division marker (Figure S11 in Supplement 1). In both non- and proinflammatory conditions in cultured or transplanted microglia, no consistent differences were observed between PD and control microglia. Finally, we immunostained transplanted microglia for p16, a cellular senescence marker. We assessed cellular senescence in cultured microglia using a cellular senescence assay kit based on β-galactosidase activity. Although a trend toward an increase in the percentage of p16-positive transplanted microglia and senescent cultured microglia was observed in PD cell lines, the differences were not statistically significant for all pairs (Figure S12 in Supplement 1). Thus, under our experimental conditions, the A53T mutation in α-synuclein did not affect apoptosis, cellular senescence, or cell division of human microglia.

Transplanted A53T Mutant Microglia Do Not Have Obvious Effects on Neighboring Murine Cells

To examine whether PD microglia affect neighboring cells, we first studied murine microglia and astrocytes neighboring transplanted human microglia. A murine cell was neighboring transplanted microglia if its cell body center was at a distance equal or inferior to 50 μm from the center of the cell body of at least 1 transplanted human microglial cell on maximum-intensity projections.

Using Iba1 immunofluorescence staining, we analyzed the morphology and distribution of murine microglia neighboring human microglia. In areas with high densities of human microglia, murine microglia were either absent or very sparse. Therefore, we analyzed areas where transplanted microglia were less dense or bordering dense patches of transplanted microglia. We found no aggregation of murine microglia around transplanted control or PD microglia (Figure S13A in Supplement 1). We categorized murine microglia neighboring the transplanted cells based on their morphology as previously described. In noninflammatory conditions, neighboring murine microglia were largely quiescent, as shown by high percentages of ramified cells (Figure S13A, B in Supplement 1). Proinflammatory conditions (LPS injection) activated murine microglia, as shown by a shift toward a less ramified morphology compared with noninflammatory conditions (Figure S13A–C in Supplement 1). No consistent differences in the morphology of murine microglia neighboring control or PD transplanted microglia were observed in non- or proinflammatory conditions (Figure S13A–C in Supplement 1).

GFAP immunofluorescence stainings showed no aggregation of murine GFAP-positive astrocytes around transplanted control or PD microglia (Figure S14A in Supplement 1). We classified murine GFAP-positive astrocytes neighboring transplanted cells into 2 morphological categories: quiescent, with a small cell body and ramified processes, and reactive, with a larger cell body and fewer, thicker processes (Figure S14B in Supplement 1). In both non- and proinflammatory conditions, the percentages of reactive GFAP-positive astrocytes were low, suggesting that in our experimental settings, LPS injection did not activate murine astrocytes (Figure S14A, C, D in Supplement 1). No consistent differences were observed in the percentage of reactive murine GFAP-positive astrocytes in the vicinity of control or PD transplanted microglia (Figure S14C, D in Supplement 1).

Next, we assessed the densities of cleaved caspase 3–positive cells in areas with a high density of transplanted human microglia (Figure S15A–C in Supplement 1). The densities of caspase 3–positive cells were low both in pro- and noninflammatory conditions, and no differences between areas with control or PD microglia were observed. We quantified oxidative stress in the vicinity of transplanted microglia by measuring the mean intensity of 8-oxo-dG/8-oxo-Gua signal in 10-μm-radius volumes of murine striatum surrounding these cells (Figure S15D–F in Supplement 1). No consistent differences in oxidative stress levels were observed between volumes surrounding PD or control microglia. Therefore, in our experimental conditions, PD microglia did not have obvious effects on the activation of neighboring murine microglia and astrocytes and did not affect apoptosis levels or oxidative stress of neighboring murine cells.

DISCUSSION

Here, we examined the impact of the A53T mutation in α-synuclein on human microglia using both traditional in vitro culture models and the transplantation of human MPs into the mouse brain. A53T mutant microglia displayed gene signatures suggesting an altered activation state, both in vitro and when transplanted in healthy, young animals, compared with isogenic control microglia. In noninflammatory conditions, transplanted striatal A53T mutant and control microglia were largely quiescent, with similar activation levels, as assessed by morphology and activation markers. However, under proinflammatory conditions induced by LPS injection in transplanted mice, striatal A53T mutant microglia displayed increased proinflammatory activation compared with control microglia. These results show that even in a young, healthy mouse brain environment, A53T mutant microglia have an intrinsically higher propensity toward proinflammatory activation. In addition, A53T mutant transplanted microglia showed decreased catalase expression and increased oxidative stress. Therefore, A53T mutant microglia display cell autonomous phenotypes that may contribute to neuronal damage in early-onset PD (Figure 6). Although no increase in apoptosis and oxidative stress was observed in the areas surrounding transplanted PD microglia, we cannot exclude more subtle effects on other indicators of neuronal health, such as neuronal activity. Furthermore, the potential deleterious effects of transplanted PD microglia on neighboring mouse neurons may be mitigated by adjacent healthy murine cells. Future investigations should explore the impact of PD microglia in mice with depleted endogenous microglia and assess their species-specific effects on human neurons in vitro.

Likewise, while we did not detect obvious effects of control or PD transplanted striatal microglia on neighboring murine microglia activation, regions densely populated with human transplanted microglia were depleted in murine microglia. This suggests competition between human and murine microglia that leads to displacement or cell death of the latter.
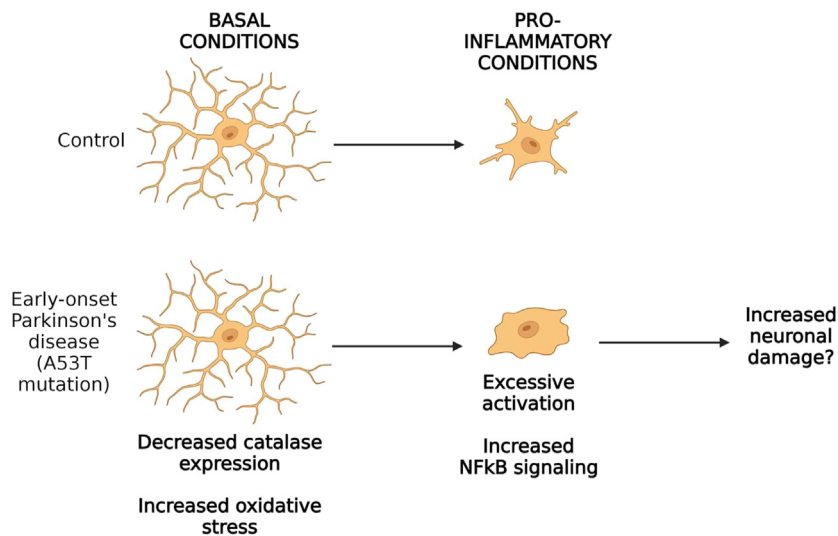
Figure 6. Cell autonomous disease–relevant phenotypes of A53T mutant human microglia. In noninflammatory conditions, A53T mutant human microglia have decreased expression of catalase and increased oxidative stress. When placed in proinflammatory conditions, A53T mutant human microglia have increased proinflammatory activation compared with control microglia, which may trigger increased neuronal damage and worsen neuronal death in patients with early-onset Parkinson's disease. NF-κB, nuclear factor-κB.

Furthermore, because we were unable to study murine microglia in areas with high densities of human transplanted microglia, we cannot exclude the possibility that the absence of difference is due to mitigation by adjacent healthy murine cells.

Although the striatum is affected in PD (25), the substantia nigra pars compacta has been the most studied, due to the early death of dopaminergic neurons in this area (33). Transplanted microglia from our cell lines did not populate this area consistently, precluding the analysis of the substantia nigra pars compacta. Future investigations should explore whether our results are recapitulated in the substantia nigra pars compacta and other brain areas using mice depleted in endogenous mouse microglia, allowing for greater integration of the transplanted cells. Here, we used immune-deprived mice lacking T, B, and natural killer cells to transplant human microglia because immunocompetent mice do not support long-term integration of these cells. While our model enables better recapitulation of human microglia's physiology, this prevents the full study of microglia–immune system interactions in PD.

Interestingly, cultured microglia from *Snca* knockout mice also show increased proinflammatory activation (34,35), suggesting that the observed effects of the A53T mutation in α-synuclein may stem from a loss of function. However, overexpression of α-synuclein in microglia also increases microglial proinflammatory activation (36,37). Because incubation with α-synuclein monomers can modulate microglia proinflammatory activation (38), and because incubation with α-synuclein aggregates triggers it (39–41), one could hypothesize that α-synuclein modulates microglia proinflammatory activation. α-synuclein overexpression may trigger the formation of α-synuclein aggregates, which may disrupt α-synuclein function, explaining similar effects between loss of function and overexpression of α-synuclein.

Mutant α-synuclein inhibits catalase expression and activity (42), and catalase activity is decreased in the brains of patients with PD and mouse models of PD (42,43). Catalase expression was strongly decreased in A53T mutant transplanted microglia

in noninflammatory conditions. Catalase is involved in the degradation of the ROS H_2O_2. Consistent with this, oxidative stress was increased in PD transplanted microglia. Surprisingly, no consistent differences in catalase expression were observed between PD and control microglia in proinflammatory conditions. This can be explained by stronger upregulation of catalase expression in PD transplanted microglia upon inflammatory stimulus compared with control microglia. While literature on the association between catalase expression and microglial activation is limited, the results of one study suggest that the NF-κB complex upregulates catalase expression (44). This could explain the increased catalase expression in PD transplanted microglia upon inflammatory stimulus because they exhibit increased proinflammatory activation, which leads to upregulation of the NF-κB pathway. In contrast, cultured control and PD microglia showed no consistent differences in catalase expression and oxidative stress, possibly due to less faithful recapitulation of microglial physiology in culture (7,8).

During activation, microglia produce and secrete ROS, including H_2O_2, which can harm neighboring cells and enhance microglial proinflammatory activation by activating the NF-κB and MAPK (mitogen-activated protein kinase) signaling pathways (45). The A53T mutation in α-synuclein may elevate intracellular ROS levels in microglia, thereby inducing increased oxidative stress and activation and triggering a vicious cycle in which microglia damage neurons and become increasingly activated via increased intracellular concentrations of ROS. In future research, we could restore catalase expression in PD microglia and assess whether this leads to decreased oxidative stress and microglial activation.

Understanding the impact of A53T mutation on microglia may shed light on the pathogenesis of PD because it provides a well-controlled way to assess the dysfunction of these cells in the inherited form of PD using isogenic hPSC pairs. However, most cases of PD are idiopathic, not inherited, and do not involve this mutation. Future research should explore the

extent to which our findings translate to idiopathic PD microglia.

ARTICLE INFORMATION

From the School of Biomedical Sciences, University of Leeds, Leeds, West Yorkshire, United Kingdom (MK); Bioinformatics and Research Computing Facility, Whitehead Institute for Biomedical Research, Cambridge, Massachusetts (BY); Wellesley College, Wellesley, Massachusetts (WC); Picower Institute for Learning and Memory, Massachusetts Institute of Technology, Cambridge, Massachusetts (TO, MS); Jaenisch laboratory, Whitehead Institute for Biomedical Research, Cambridge, Massachusetts (DF, CMG-E, KRA, MDG, RJ); and Shoreline Biosciences Inc., San Diego, California (DSS).

Address correspondence to Marine Krzisch, Ph.D., at m.krzisch@leeds.ac.uk, or Rudolf Jaenisch, M.D., at jaenisch@wi.mit.edu.

Received Sep 18, 2023; revised Jun 8, 2024; accepted Jul 3, 2024.

Supplementary material cited in this article is available online at https://doi.org/10.1016/j.biopsych.2024.07.011.

REFERENCES

1. Bartels AL, Willemsen AT, Doorduin J, de Vries EF, Dierckx RA, Leenders KL (2010): [11C]-PK11195 PET: Quantification of neuro-inflammation and a monitor of anti-inflammatory treatment in Parkinson's disease? Parkinsonism Relat Disord 16:57–59.

2. Gerhard A, Pavese N, Hotton G, Turkheimer F, Es M, Hammers A, et al. (2006): In vivo imaging of microglial activation with [11C](R)-PK11195 PET in idiopathic Parkinson's disease. Neurobiol Dis 21:404–412.

3. Polymeropoulos MH, Lavedan C, Leroy E, Ide SE, Dehejia A, Dutra A, et al. (1997): Mutation in the alpha-synuclein gene identified in families with Parkinson's disease. Science 276:2045–2047.

4. Hoenen C, Gustin A, Birck C, Kirchmeyer M, Beaume N, Felten P, et al. (2016): Alpha-synuclein proteins promote pro-inflammatory cascades in microglia: Stronger effects of the A53T mutant. PLoS One 11: e0162717.

5. Potashkin JA, Blume SR, Runkle NK (2010): Limitations of animal models of Parkinson's disease. Parkinsons Dis 2011:658083.

6. Geirsdottir L, David E, Keren-Shaul H, Weiner A, Bohlen SC, Neuber J, et al. (2020): Cross-species single-cell analysis reveals divergence of the primate microglia program. Cell 181:746.

7. Gosselin D, Skola D, Coufal NG, Holtman IR, Schlachetzki JCM, Sajti E, et al. (2017): An environment-dependent transcriptional network specifies human microglia identity. Science 356.

8. Bohlen CJ, Bennett FC, Tucker AF, Collins HY, Mulinyawe SB, Barres BA (2017): Diverse requirements for microglial survival, specification, and function revealed by defined-medium cultures. Neuron 94:759–773.e8.

9. Xu R, Li X, Boreland AJ, Posyton A, Kwan K, Hart RP, Jiang P (2020): Human iPSC-derived mature microglia retain their identity and functionally integrate in the chimeric mouse brain. Nat Commun 11:1577.

10. Svoboda DS, Barrasa MI, Shu J, Rietjens R, Zhang S, Mitalipova M, et al. (2019): Human iPSC-derived microglia assume a primary microglia-like state after transplantation into the neonatal mouse brain. Proc Natl Acad Sci U S A 116:25293–25303.

11. Hasselmann J, Coburn MA, England W, Figueroa Velez DX, Kiani Shabestari S, Tu CH, et al. (2019): Development of a chimeric model to study and manipulate human microglia in vivo. Neuron 103:1016–1033.e10.

12. Mancuso R, Van Den Daele J, Fattorelli N, Wolfs L, Balusu S, Burton O, et al. (2019): Stem-cell-derived human microglia transplanted in mouse brain to study human disease. Nat Neurosci 22:2111–2116.

13. Soldner F, Laganière J, Cheng AW, Hockemeyer D, Gao Q, Alagappan R, et al. (2011): Generation of isogenic pluripotent stem cells differing exclusively at two early onset Parkinson point mutations. Cell 146:318–331.

14. Ma H, Wert KJ, Shvartsman D, Melton DA, Jaenisch R (2018): Establishment of human pluripotent stem cell-derived pancreatic beta-like cells in the mouse pancreas. Proc Natl Acad Sci U S A 115:3924–3929.

15. McQuade A, Coburn M, Tu CH, Hasselmann J, Davtyan H, Blurton-Jones M (2018): Development and validation of a simplified method to generate human microglia from pluripotent stem cells. Mol Neurodegener 13:67.

16. Brownjohn PW, Smith J, Solanki R, Lohmann E, Houlden H, Hardy J, et al. (2018): Functional studies of missense TREM2 mutations in human stem cell-derived microglia. Stem Cell Rep 10:1294–1307.

17. Markopoulou K, Wszolek ZK, Pfeiffer RF, Chase BA (1999): Reduced expression of the G209A alpha-synuclein allele in familial Parkinsonism. Ann Neurol 46:374–381.

18. Voutsinas GE, Stavrou EF, Karousos G, Dasoula A, Papachatzopoulou A, Syrrou M, et al. (2010): Allelic imbalance of expression and epigenetic regulation within the alpha-synuclein wild-type and p.Ala53Thr alleles in Parkinson disease. Hum Mutat 31:685–691.

19. Haenseler W, Zambon F, Lee H, Vowles J, Rinaldi F, Duggal G, et al. (2017): Excess alpha-synuclein compromises phagocytosis in iPSC-derived macrophages. Sci Rep 7:9003.

20. Booms A, Coetzee GA (2021): Functions of intracellular alpha-synuclein in microglia: Implications for Parkinson's disease risk. Front Cell Neurosci 15:759571.

21. Nandi A, Yan LJ, Jana CK, Das N (2019): Role of catalase in oxidative stress- and age-associated degenerative diseases. Oxid Med Cell Longev 2019:9613090.

22. Ryu HS, Park KW, Choi N, Kim J, Park YM, Jo S, et al. (2020): Genomic analysis identifies new loci associated with motor complications in Parkinson's disease. Front Neurol 11:570.

23. Smajić S, Prada-Medina CA, Landoulsi Z, Ghelfi J, Delcambre S, Dietrich C, et al. (2022): Single-cell sequencing of human midbrain reveals glial activation and a Parkinson-specific neuronal state. Brain 145:964–978.

24. Jurga AM, Paleczna M, Kuter KZ (2020): Overview of general and discriminating markers of differential microglia phenotypes. Front Cell Neurosci 14:198.

25. Zhai S, Tanimura A, Graves SM, Shen W, Surmeier DJ (2018): Striatal synapses, circuits, and Parkinson's disease. Curr Opin Neurobiol 48:9–16.

26. Lier J, Streit WJ, Bechmann I (2021): Beyond activation: Characterizing microglial functional phenotypes. Cells 10.

27. Liu T, Zhang L, Joo D, Sun S-C (2017): NF-κB signaling in inflammation. Signal Transduct Target Ther 2:17023.

28. Singh SS, Rai SN, Birla H, Zahra W, Rathore AS, Singh SP (2020): NF-κB-mediated neuroinflammation in Parkinson's disease and potential therapeutic effect of polyphenols. Neurotox Res 37:491–507.

29. Frakes AE, Ferraiuolo L, Haidet-Phillips AM, Schmelzer L, Braun L, Miranda CJ, et al. (2014): Microglia induce motor neuron death via the classical NF-κB pathway in amyotrophic lateral sclerosis. Neuron 81:1009–1023.

30. Jonas RA, Yuan TF, Liang YX, Jonas JB, Tay DKC, Ellis-Behnke RG (2012): The spider effect: Morphological and orienting classification of microglia in response to stimuli in vivo. PLoS One 7:e30763.

31. Franco-Bocanegra DK, Gourari Y, McAuley C, Chatelet DS, Johnston DA, Nicoll JAR, Boche D (2021): Microglial morphology in Alzheimer's disease and after Aβ immunotherapy. Sci Rep 11:15955.

32. Deng I, Corrigan F, Zhai G, Zhou XF, Bobrovskaya L (2020): Lipopolysaccharide animal models of Parkinson's disease: Recent progress and relevance to clinical disease. Brain Behav Immun Health 4:100060.

33. Poewe W, Seppi K, Tanner CM, Halliday GM, Brundin P, Volkmann J, et al. (2017): Parkinson disease. Nat Rev Dis Primers 3:17013.

34. Austin SA, Rojanathammanee L, Golovko MY, Murphy EJ, Combs CK (2011): Lack of alpha-synuclein modulates microglial phenotype in vitro. Neurochem Res 36:994–1004.

35. Austin SA, Floden AM, Murphy EJ, Combs CK (2006): Alpha-synuclein expression modulates microglial activation phenotype. J Neurosci 26:10558–10563.

36. Bido S, Muggeo S, Massimino L, Marzi MJ, Giannelli SG, Melacini E, et al. (2021): Microglia-specific overexpression of alpha-synuclein leads to severe dopaminergic neurodegeneration by phagocytic exhaustion and oxidative toxicity. Nat Commun 12:6237.

37. Rojanathammanee L, Murphy EJ, Combs CK (2011): Expression of mutant alpha-synuclein modulates microglial phenotype in vitro. J Neuroinflammation 8:44.

38. Li N, Stewart T, Sheng L, Shi M, Cilento EM, Wu Y, et al. (2020): Immunoregulation of microglial polarization: An unrecognized physiological function of alpha-synuclein. J Neuroinflammation 17:272.

39. Wilms H, Rosenstiel P, Romero-Ramos M, Arlt A, Schäfer H, Seegert D, et al. (2009): Suppression of MAP kinases inhibits microglial activation and attenuates neuronal cell death induced by alpha-synuclein protofibrils. Int J Immunopathol Pharmacol 22:897–909.

40. Long H, Zhang S, Zeng S, Tong Y, Liu J, Liu C, Li D (2022): Interaction of RAGE with alpha-synuclein fibrils mediates inflammatory response of microglia. Cell Rep 40:111401.

41. Zhang W, Wang T, Pei Z, Miller DS, Wu X, Block ML, et al. (2005): Aggregated alpha-synuclein activates microglia: A process leading to disease progression in Parkinson's disease. FASEB J 19:533–542.

42. Yakunin E, Kisos H, Kulik W, Grigoletto J, Wanders RJA, Sharon R (2014): The regulation of catalase activity by PPAR gamma is affected by α-synuclein. Ann Clin Transl Neurol 1:145–159.

43. Ambani LM, Van Woert MH, Murphy S (1975): Brain peroxidase and catalase in Parkinson disease. Arch Neurol 32:114–118.

44. Zhou LZ, Johnson AP, Rando TA (2001): NF kappa B and AP-1 mediate transcriptional responses to oxidative stress in skeletal muscle cells. Free Radic Biol Med 31:1405–1416.

45. Bordt EA, Polster BM (2014): NADPH oxidase- and mitochondria-derived reactive oxygen species in proinflammatory microglial activation: A bipartisan affair? Free Radic Biol Med 76:34–46.